A VUV Photoionization and Ab Initio Determination of the Ionization Energy of a Gas Phase Sugar (Deoxyribose)

Debashree Ghosh[1], Amir Golan[2], Lynelle K. Takahashi[2,3], Anna Krylov[1], and Musahid Ahmed[2*]

[1]Department of Chemistry, University of Southern California, Los Angeles, CA 90089-0482

[2]Chemical Sciences Division, Lawrence Berkeley National Laboratory, Berkeley, CA 94720

[3]Department of Chemistry, University of California at Berkeley, Berkeley, CA 94720

Supplementary Material

The supplementary materials contains:

1. Total energies of the different isomers of deoxyribose (DFT/ωB97x/cc-pVTZ).
2. Electronic structure analysis of the deoxyribose cation.
3. Calculation of the water elimination fragmentation channel.
4. Movie of a water elimination event.
5. Fragments observed in ab initio molecular dynamics (AIMD) calculations.
6. Calculated ionization spectra and photoionization efficiency curve.
7. Experimental details and photoionization efficiency curves of major fragments.
8. Optimized geometries of 2-deoxy-D-ribose.

1. Total energy of different isomers of deoxyribose (DFT/ωB97x/cc-pVTZ)

Species	Energy in Hartrees
Furanose	-497.495019
α-Pyranose	-497.507616
β-Pyranose	-497.498693
Ribose	-497.491261

2. Electronic structure of the α-pyranose cation.

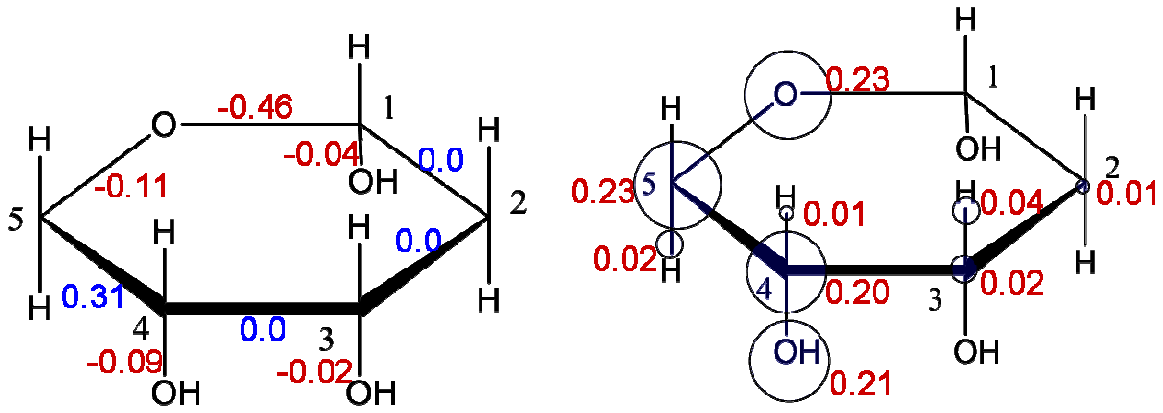

Figure S1. (a) The structural differences between the cationic and neutral α pyranose form of deoxyribose, in angstroms. (b) The distribution of the spin density (unpaired electron) in the cationic α-pyranose.

The structural differences between the neutral and the cationic form of the deoxyribose are shown in Fig. S1. We see that the major differences are: the C_4-C_5 bond elongation and the O-C_1 bond contraction, followed by the C_5-O bond shortening. The spin density shows that there is significant spin density on the ring O atom and oxygen bonded to C_4, as well as the C_4 and C_5 atoms. The distribution of the spin density is following the shape of the MO from which the ionization occurs. This is consistent with Koopmans character of the ionized states revealed by EOM-IP-CCSD amplitudes.

3. Water elimination fragmentation channel

The detailed picture of the energy and the free energy of the deoxyribose along the water elimination channel is given in Fig. S2. We notice that water elimination occurs with opening up of the pentose ring in the C_4-C_5 bond (which is 1.84 angstroms in the cationic species). The TS is an open-chain deoxyribose, followed by water elimination. As expected for a fragmentation process, the effect of entropy change during the reaction pathway is significant. This is seen from the difference between the energy and free energy values along the reaction coordinate. However, it should be noted that while the entropy contribution can be quantitatively evaluated for the reactant, transition state, and product structures, the other points along the reaction coordinate the computed entropic effects are of a qualitative value only.

Computational procedures:

(i) AIMD/B3LYP/6-31+G* calculations at 300 K (Q-Chem) starting from a cation structure that is slightly displaced along the most active normal modes.

(ii) Few snapshots are taken from the trajectories and optimized (ωB97x/cc-pVTZ) keeping the C_4-C_5 bond length fixed (in the first part of the trajectory, when the pentose ring breaks).

(iii) Few snapshots are taken from the trajectories and optimized (ωB97x/cc-pVTZ) keeping the C_3O-H bond length fixed (in the first part of the trajectory, where the H abstraction occurs).

(iv) Entropy calculated for each of the optimized geometry within RRHO approximation.

(v) Energy and free energy of the optimized species are plotted.

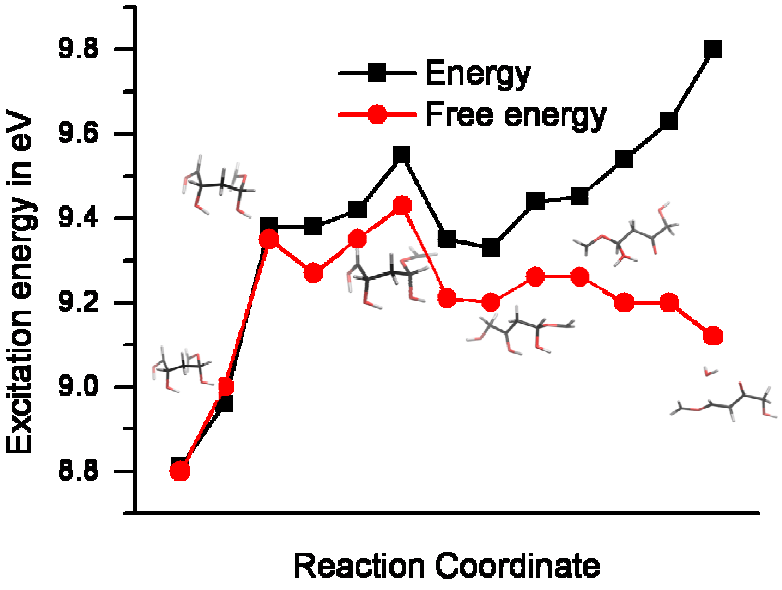

Figure S2: The free and potential energy values of the constrained optimized geometry of deoxyribose along the water elimination channel. In the first part of the reaction coordinate, the C_4-C_5 bond length is constrained, whereas in the second part, the O-H bond of the C_1 is constrained.

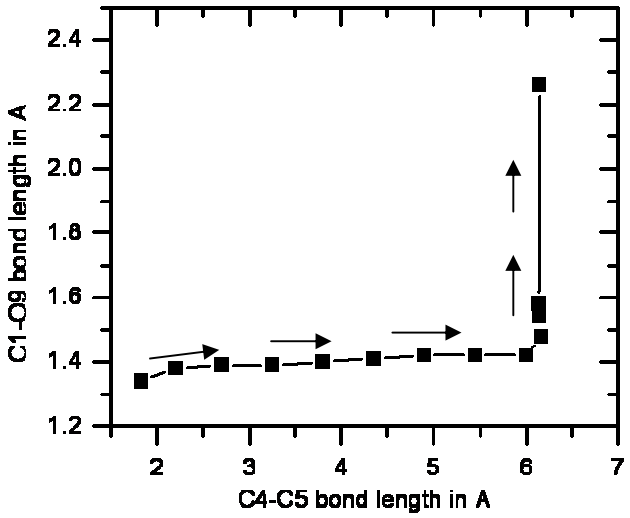

Figure S3: The C_4-C_5 and C_1-OH bond lengths along the reaction coordinate. Snapshots taken from AIMD simulation with the B3LYP functional and the 6-31+G(d) basis set.

Fig. S3 shows the change in the C_4-C_5 and C_1-OH bond lengths along the reaction coordinate. This explains the nature of the reaction coordinate. We notice that in the first part of the process the only major change is in the C_4-C_5 bond length (where the bond breaks and ring unfurls). The later part consists of change in C_1-O_9 and C_3O-H bond length (when the H abstraction and water elimination occurs). The arrows in Fig. S3 show the direction of the trajectory.

To confirm the TS structure and reaction barrier, the TS was optimized without any constraints (see Fig. S4).

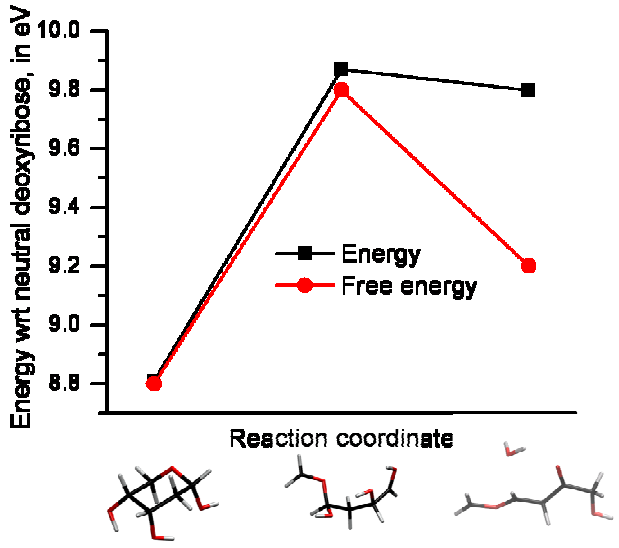

Figure S4: Energy and free energy calculated for the deoxyribose cation, m/z 116 fragment + H_2O and the TS. The TS geometry is obtained by transition state optimization (with no constraints) at the ωB97x/cc-PVTZ level of theory.

4. Movie of a water elimination event

The movie presents AIMD snapshots of a trajectory leading to H_2O elimination. The trajectory is computed using constant energy ensemble with initial kinetic energy of 300 K. The trajectories are run for 4 ps with a 2 fs time step. The snapshots are taken each 100 fs for the first 2.5-3 ps. The movie shows the major events in the reaction:

(i) C_4-C_5 bond elongation and breaking.

(ii) The pentose ring breaking and unfurling, C_1-OH and C_3-OH are approaching each other.

(iii) C_3O-H and C_1-O bond elongation.

(iv) Water elimination by H abstraction from C_3 and OH abstraction from C_1.

5. Fragments observed in AIMD calculations.

The dominant channel is water elimination leading to m/z=134 fragment:

CH_2OH-CO-CH_2-CH-O-CH_2.

The CH_2O elimination produces m/z=104: CHOH-CH_2-CHOH-CHOH.

The fragments with m/z=86, 60, and 44 are produced by secondary fragmentation of m/z=104 (formaldehyde elimination) and have the following chemical structures:

86: $CHOH=CH-CH_2-CH_2$

60: CHOH=CHOH (cis and trans isomers)

44: $CH_2=CH_2OH$

6. Calculated ionization spectra and photoionization efficiency curve.

Fig. S5 shows the assigned photoelectron spectrum and the integrated PIE curve. It should be noted that the calculated PIE curve does not agree well with the experimental observation. The main reason for this discrepancy could arise from the anharmonicity and the non-rigidity of the pyranose framework. Note that computed difference between 00 transition and the apparent PIE onset is about 0.05-0.1 eV.

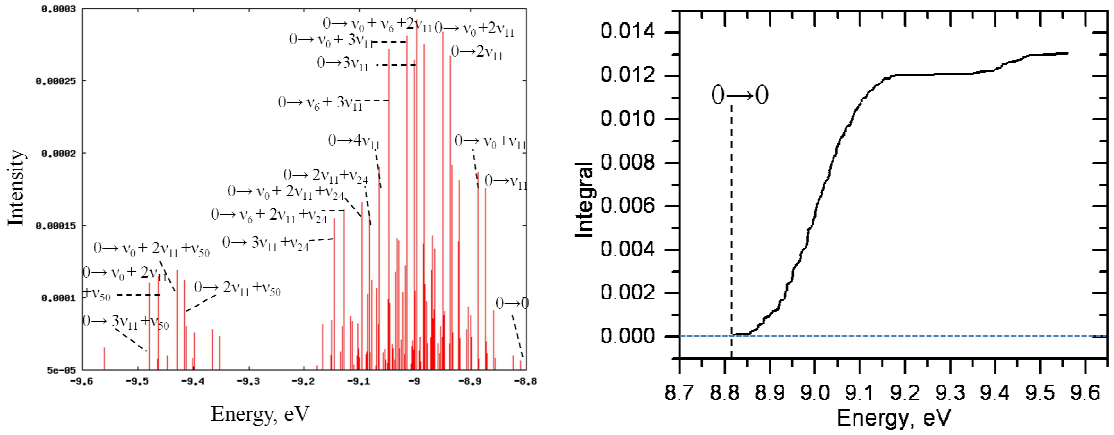

Figure S5. The calculated ionization spectrum and the integrated PIE curve computed within double-harmonic approximation using the ezSpectrum software.

7. Experimental details and photoionization efficiency curves of major fragments.

The experiment was performed on an effusive thermal desorption apparatus coupled to a 3 m VUV monochromator on the Chemical Dynamics Beamline at the Advanced Light Source. We placed the sample in a heated aluminum oven attached to the repeller plate of a commercial reflectron mass spectrometer (R. M. Jordan) allowing vapors to pass through a 1mm pinhole in

the plate and reach the interaction region of the mass spectrometer. The effusive molecular source was then interrogated by tunable, monochromatized synchrotron undulator VUV radiation (see Fig. S6). The photoionization region was situated 5 mm from the oven pinhole. As the synchrotron light is quasi-continuous (500 MHz), a start pulse for the TOF ion packet was provided by pulsing the electrical fields of the ion optics. In general, the ion optics were biased in such a fashion that all positive ions were accelerated away from the detector until the start pulse occurred. Ion signals from the microchannel plate detector were amplified by pre-amplifier (ORTEC VT120A) and then collected with a multichannel-scalar card (FAST Comtec 7886). Time-of-flight spectra were recorded for the photoionization energy range between 8 eV and 11 eV. The typical step size of the VUV photon energy used for these experiments was 50 meV, and the data collection time at each of these energy steps was 60 s. The PIE curves of the parent sample and its fragments (see Fig. S7) were obtained by adding all of the ion counts in the mass peak at each photon energy, normalized by the photon flux. The synchrotron VUV photon flux was measured by a Si photodiode (International Radiation Detectors, SXUV-100).

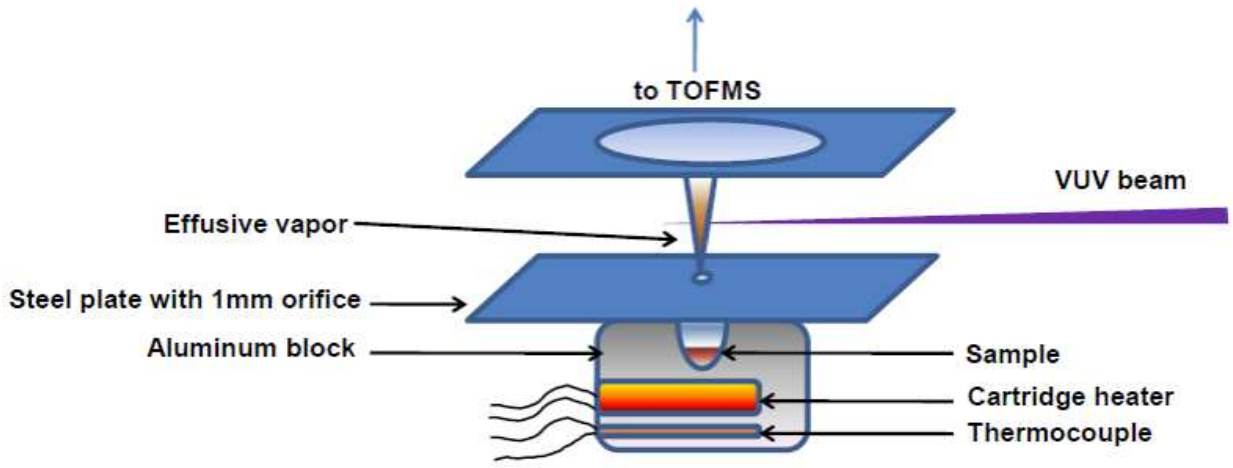

Figure S6. A schematic diagram of the effusive source showing the oven attached to the bottom of the first (repeller) plate of the time-of-flight mass spectrometer.

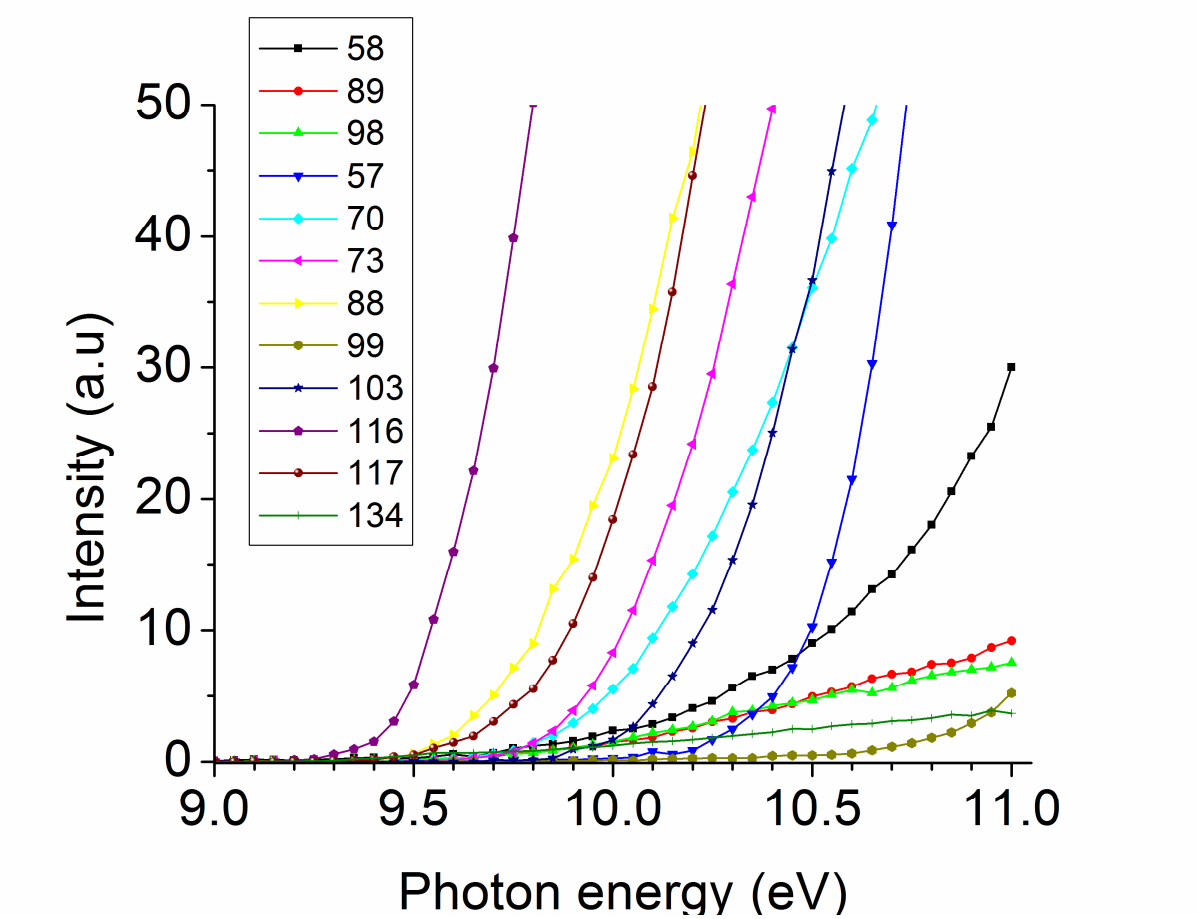

Figure S7. The PIE curves of major fragments in deoxyribose photoionization recorded with an effusive source.

8. Optimized geometries of 2-deoxy-D-ribose

A. Optimized geometry of pyranose α-deoxy-D-ribose

C	1.617006	-0.145521	-0.328544
C	0.778510	0.898493	-1.049855
C	-0.636253	0.962489	-0.490056
C	-1.241464	-0.439640	-0.454905
C	-0.306717	-1.393079	0.278495
O	0.999966	-1.400822	-0.290301
O	-2.503813	-0.423993	0.166150
O	-0.686990	1.535332	0.810504
O	1.870984	0.345960	0.977749
H	2.561857	-0.317070	-0.849246
H	1.260410	1.873532	-0.979889
H	0.735480	0.616062	-2.102920

H	-1.381458	-0.793164	-1.479843
H	-0.678370	-2.413028	0.216710
H	-0.265544	-1.108983	1.335357
H	-2.430825	0.198279	0.898392
H	0.117539	1.283983	1.277703
H	2.385349	-0.312817	1.449639
H	-1.263019	1.597888	-1.117866

B. Optimized geometry of furanose deoxy-D-ribose

O	-2.785824	-0.991028	0.255410
C	-2.055023	0.093341	-0.271463
C	-0.605075	0.056393	0.141328
O	-0.008593	-1.108221	-0.422348
C	0.245919	1.201053	-0.392087
O	0.157844	2.288049	0.505138
C	1.640376	0.568343	-0.511841
C	1.391364	-0.936528	-0.389841
O	1.938636	-1.373098	0.825105
H	-2.324065	-1.793581	0.003415
H	-2.108557	0.113489	-1.367765
H	-2.508423	1.007225	0.114284
H	-0.527675	0.035515	1.233901
H	-0.126196	1.497187	-1.380301
H	0.570117	3.055053	0.107202
H	2.133266	0.819032	-1.449537
H	1.787003	-1.524353	-1.221665
H	1.736334	-2.306040	0.921905
H	2.266685	0.896704	0.316060

C. Optimized geometry of pyranose β-deoxy-D-ribose

C	1.485335	0.052563	0.218546
C	0.721229	1.080751	-0.595168
C	-0.781971	0.948377	-0.398127
C	-1.227761	-0.508615	-0.537503
C	-0.334535	-1.415960	0.302644
O	1.025444	-1.253495	-0.050269
O	-2.577951	-0.656447	-0.170946
O	-1.217488	1.456319	0.865023
O	2.823337	0.128099	-0.130571
H	1.049679	2.085771	-0.327529
H	0.978205	0.908743	-1.642162
H	-1.134828	-0.808102	-1.584341
H	-0.591897	-2.459762	0.136576
H	-0.485973	-1.201374	1.372239

H	-2.729624	-0.035847	0.549814
H	-0.596972	1.194592	1.547318
H	-1.316647	1.552752	-1.131104
H	3.291235	-0.571556	0.330863
H	1.360599	0.230359	1.304880

D. Optimized geometry of cationic pyranose α-deoxy-D-ribose

C	-1.637045	0.209635	-0.280803
C	-0.813760	-0.772792	-1.096466
C	0.591686	-0.944274	-0.548320
C	1.389802	0.359809	-0.456473
C	0.226210	1.482594	0.396426
O	-0.895144	1.465733	-0.304241
O	2.460096	0.301372	0.312955
O	0.688233	-1.579321	0.699247
O	-1.784828	-0.262958	1.006513
H	-2.583061	0.463666	-0.753783
H	-1.316883	-1.739085	-1.104480
H	-0.763966	-0.415869	-2.125159
H	1.570601	0.919403	-1.372931
H	0.733063	2.440128	0.341585
H	0.202794	0.988232	1.366693
H	2.329637	-0.413657	0.966021
H	-0.148704	-1.523460	1.173787
H	-2.542825	0.133547	1.445452
H	1.166464	-1.550153	-1.260781

E. Optimized geometry of transition state (m/z=116 pathway)

C	-1.305847	-0.524517	-0.409140
C	-0.007062	-0.539434	-1.201500
C	1.259077	-0.560931	-0.280966
C	2.228095	0.424349	-0.807128
C	-2.750937	1.032150	0.551886
O	-1.494247	0.775557	0.080297
O	2.567423	1.372798	-0.073492
O	1.090012	-0.176150	1.049737
O	-1.183276	-1.456834	0.634972
H	-2.142785	-0.792053	-1.063219
H	0.018546	-1.424993	-1.832469
H	-0.028077	0.336026	-1.850944
H	2.657149	0.391419	-1.806118
H	-3.580713	0.534808	0.060439

H	-2.856343	2.003400	1.006207
H	2.080257	1.245096	0.794842
H	0.265251	-0.560410	1.391270
H	-2.034197	-1.588681	1.063844
H	1.729782	-1.550533	-0.355294

F. Constrained optimized geometries along the pathway for water abstraction

C_4-C_5 = 1.7 Å

C	-1.659059	-0.074203	-0.283331
C	-0.672064	-0.881553	-1.106182
C	0.755722	-0.884408	-0.568251
C	1.430777	0.471138	-0.509979
C	-0.196292	1.635952	0.404271
O	-1.228989	1.322160	-0.332448
O	2.420215	0.591955	0.323260
O	0.930319	-1.495205	0.686957
O	-1.685589	-0.546227	1.014253
H	-2.645760	-0.049128	-0.740141
H	-1.027380	-1.910825	-1.146558
H	-0.672969	-0.495085	-2.125910
H	1.497942	1.108277	-1.386902
H	0.161110	2.649304	0.269701
H	-0.067595	1.143891	1.364004
H	2.367156	-0.145433	0.965349
H	0.100455	-1.487018	1.177387
H	-2.518445	-0.344615	1.449700
H	1.367886	-1.454554	-1.280999

C_4-C_5 = 2.2 Å

C	-1.635689	-0.062418	-0.254876
C	-0.644787	-0.829586	-1.117469
C	0.789729	-0.935666	-0.602291
C	1.607519	0.326674	-0.551012
C	-0.404606	1.839450	0.425133
O	-1.366885	1.352571	-0.335713
O	2.500579	0.405332	0.353313
O	0.944610	-1.574106	0.640723
O	-1.568415	-0.531756	1.050082
H	-2.638456	-0.148740	-0.669726
H	-1.020328	-1.848371	-1.213390
H	-0.642490	-0.391518	-2.115747
H	1.686979	1.035445	-1.368698
H	-0.160176	2.873350	0.225977
H	-0.217880	1.390156	1.393280

H	2.348008	-0.345968	0.975881
H	0.129998	-1.477770	1.152559
H	-2.389855	-0.377681	1.524499
H	1.339587	-1.544974	-1.338345

C_4-C_5 = 2.7 Å

C	1.410997	-0.238368	-0.178510
C	0.976475	0.971669	-0.980235
C	-0.474244	1.243660	-0.606131
C	-1.217081	-0.074429	-0.697946
C	0.017818	-2.135853	0.533133
O	0.250422	-1.133763	-0.356978
O	-2.093465	-0.331006	0.210169
O	-0.676480	1.752869	0.688435
O	1.571608	0.098577	1.144358
H	2.264821	-0.774357	-0.589151
H	1.615719	1.825083	-0.766449
H	1.042717	0.750798	-2.045752
H	-1.413750	-0.529464	-1.661726
H	-0.723821	-2.853538	0.226715
H	0.403935	-2.042186	1.535009
H	-1.970609	0.318757	0.935070
H	0.099763	1.596085	1.237319
H	2.241859	-0.434756	1.578963
H	-0.935213	1.933725	-1.317347

C_4-C_5 = 3.25 Å

C	1.253637	0.601479	-0.353928
C	0.060437	1.305242	-0.969532
C	-1.224341	0.737405	-0.372810
C	-1.294287	-0.748574	-0.561944
C	1.740877	-1.703475	0.100205
O	0.963375	-0.789547	-0.546464
O	-1.652616	-1.456734	0.414719
O	-1.418669	0.976721	0.998017
O	1.319821	0.924740	0.999255
H	2.190267	0.824440	-0.866298
H	0.108580	2.375750	-0.781441
H	0.059097	1.150969	-2.048626
H	-1.245472	-1.234894	-1.529446
H	1.670858	-2.706344	-0.285079
H	2.132979	-1.455189	1.074397

H	-1.728405	-0.845782	1.194510
H	-0.569041	1.185782	1.411590
H	2.223105	0.952539	1.322083
H	-2.085994	1.146727	-0.916182

C_4-C_5 = 3.8 Å

C	1.227370	0.565680	-0.346837
C	0.027609	1.110178	-1.095615
C	-1.287885	0.684531	-0.442375
C	-1.507455	-0.792609	-0.448493
C	2.179047	-1.545366	0.083543
O	1.059791	-0.835940	-0.278737
O	-1.906279	-1.323511	0.607953
O	-1.477619	1.102340	0.883117
O	1.217559	1.140972	0.929532
H	2.162259	0.788479	-0.869361
H	0.064055	2.197583	-1.113217
H	0.049161	0.752718	-2.125157
H	-1.430093	-1.428022	-1.326516
H	3.134680	-1.156019	-0.247274
H	2.005500	-2.599700	0.223964
H	-1.928063	-0.587817	1.289189
H	-0.607893	1.307470	1.268267
H	2.023753	0.935835	1.411311
H	-2.112825	1.078762	-1.056076

C_4-C_5 = 4.35 Å

C	1.304367	0.308458	-0.362661
C	0.175065	1.059345	-1.049637
C	-1.192773	0.955159	-0.356878
C	-1.935510	-0.315487	-0.589327
C	2.095217	-1.876510	-0.100505
O	1.011335	-1.064778	-0.349776
O	-2.418497	-0.890277	0.404147
O	-1.206120	1.152194	1.029317
O	1.410639	0.823297	0.941191
H	2.239447	0.469503	-0.909571
H	0.446856	2.113225	-1.075793
H	0.091826	0.714416	-2.080468
H	-2.137837	-0.749222	-1.566102
H	3.057705	-1.537218	-0.466126
H	1.843278	-2.920900	-0.019210

H	-2.127465	-0.339102	1.196001
H	-0.286457	1.126224	1.357896
H	2.157549	0.428547	1.401135
H	-1.845285	1.705565	-0.836346

C_4-C_5 = 4.9 Å

C	-1.404888	-0.106470	-0.686843
C	-0.019600	-0.333369	-1.273809
C	0.980097	-0.351940	-0.167829
C	2.220124	0.454489	-0.253158
C	-2.486606	1.585579	0.506658
O	-1.303623	1.071527	0.052687
O	3.051674	0.360624	0.840592
O	0.772424	-1.021398	0.874720
O	-1.661649	-1.224663	0.142335
H	-2.174629	-0.020451	-1.458450
H	0.017396	-1.305099	-1.773737
H	0.226065	0.441404	-1.996537
H	1.842186	1.486678	-0.323880
H	-2.366894	2.412372	1.186457
H	-3.353655	1.478128	-0.136198
H	3.665087	-0.372147	0.753541
H	-0.163561	-1.383913	0.864959
H	-2.507986	-1.128041	0.593098
H	2.692138	0.253772	-1.225204

C_4-C_5 = 5.45 Å

C	-1.395717	-0.210189	-0.602179
C	0.014911	-0.286579	-1.172325
C	1.089235	-0.262121	-0.136944
C	2.434925	0.289428	-0.461427
C	-2.854317	1.379337	0.272410
O	-1.558783	1.049896	-0.039063
O	3.315599	0.202086	0.596349
O	0.898191	-0.718844	1.013895
O	-1.481604	-1.229009	0.383842
H	-2.145336	-0.387230	-1.378671
H	0.136847	-1.237542	-1.703527
H	0.177663	0.509888	-1.896533
H	2.246541	1.340461	-0.734793
H	-2.941937	2.304046	0.818294
H	-3.627702	1.033930	-0.405891

H	4.076177	-0.336811	0.374490
H	-0.059045	-1.032391	1.099206
H	-2.343352	-1.205450	0.815240
H	2.769172	-0.193115	-1.388783

C_4-C_5 = 6.0 Å

C	-1.375581	0.074781	-0.667742
C	0.029817	0.691084	-0.806198
C	1.171885	0.049795	-0.082747
C	2.555055	0.660506	-0.100314
C	-3.422156	0.474063	0.387732
O	-2.054712	0.668886	0.388305
O	3.530055	-0.174379	0.398313
O	1.043323	-1.039441	0.521585
O	-1.207810	-1.319434	-0.449755
H	-1.933028	0.223090	-1.597974
H	0.325356	0.688194	-1.860533
H	-0.010107	1.743685	-0.516842
H	2.481029	1.637336	0.397435
H	-3.902204	0.853586	1.274038
H	-3.912230	0.441270	-0.579190
H	3.615237	-0.085654	1.349967
H	0.102998	-1.397766	0.377079
H	-2.061035	-1.740668	-0.296220
H	2.777907	0.880490	-1.151070

O_8-H_{17}=1.25 Å

C	-1.190110	0.057029	0.116254
C	0.161646	-0.512057	-0.276370
C	1.314341	0.432895	-0.122873
C	2.713499	-0.089029	-0.080783
C	-3.439841	-0.495511	0.034449
O	-2.179205	-0.645900	-0.494190
O	2.679899	-1.483498	-0.101349
O	1.135170	1.655406	-0.064161
O	-1.203546	1.456639	-0.373574
H	-1.326890	0.105804	1.201110
H	0.363150	-1.425832	0.281597
H	0.139091	-0.816815	-1.328478
H	3.177431	0.330163	0.821156
H	-4.205777	-0.970020	-0.555780

H	-3.511650	-0.390541	1.111611
H	3.570517	-1.837651	-0.130663
H	-0.096527	1.820002	-0.199548
H	-1.931262	1.971752	-0.002746
H	3.229975	0.349590	-0.944314

O_8-H_{17}=1.5 Å

C	1.166953	0.068694	0.233252
C	-0.200474	0.522978	-0.215173
C	-1.304413	-0.477446	0.032406
C	-2.723620	0.009481	0.056369
C	3.382286	0.746287	0.267096
O	2.138485	0.814368	-0.322670
O	-2.729940	1.406521	-0.006322
O	-1.067304	-1.669517	0.176108
O	1.317530	-1.365247	-0.300212
H	1.264691	-0.031296	1.317957
H	-0.443578	1.464416	0.276817
H	-0.180938	0.744792	-1.286758
H	-3.182307	-0.392069	0.966968
H	4.141413	1.265312	-0.293393
H	3.409287	0.650002	1.346698
H	-3.630902	1.733291	-0.029246
H	0.402484	-1.817152	-0.084517
H	2.088390	-1.825716	0.061792
H	-3.224154	-0.462570	-0.798377

O_8-H_{17}=1.75 Å

C	-1.089124	-0.051463	0.251762
C	0.240654	-0.486471	-0.294168
C	1.361650	0.504764	-0.061079
C	2.775095	-0.005450	-0.129957
C	-3.283368	-0.731164	0.520385
O	-2.091638	-0.834643	-0.165831
O	2.752879	-1.398365	-0.277071
O	1.143473	1.682181	0.156307
O	-1.362610	1.371611	-0.371284
H	-1.098046	0.146035	1.326654
H	0.503592	-1.443412	0.158561
H	0.160155	-0.679329	-1.367815
H	3.278426	0.329800	0.783420

H	-4.092384	-1.261746	0.046894
H	-3.223808	-0.579036	1.592225
H	3.645918	-1.736463	-0.360073
H	-0.558936	1.927981	-0.166011
H	-2.184158	1.766838	-0.040721
H	3.251576	0.505431	-0.975199

O_8-H_{17}=2.0 Å

C	-1.103949	-0.457624	0.341863
C	0.254632	-0.673282	-0.173641
C	1.289425	0.276506	0.418914
C	2.733251	-0.047936	0.128839
C	-3.366145	-0.800002	0.082554
O	-2.080155	-0.931703	-0.328669
O	2.787375	-1.186014	-0.690402
O	0.976506	1.229446	1.088218
O	-1.511385	1.744752	0.052131
H	-1.285454	-0.110443	1.354238
H	0.549676	-1.700399	0.083036
H	0.279971	-0.648430	-1.264277
H	3.225491	-0.190594	1.097362
H	-4.079105	-1.294099	-0.552877
H	-3.562343	-0.240945	0.985113
H	3.698899	-1.416856	-0.875242
H	3.174300	0.839743	-0.336612
H	-0.732370	2.091748	0.508411
H	-1.630408	2.268382	-0.744405